The Structure of Zinc Chloride Complexes in Aqueous Solution

M. Maeda a. T. Ito a. M. Hori a. and G. Johansson b

- ^a Department of Applied Chemistry, Nagoya Institute of Technology, Gokiso-cho, Showa-ku, Nagoya 466, Japan
- b Department of Inorganic Chemistry, Royal Institute of Technology, S-100 44 Stockholm, Sweden
- Z. Naturforsch. **51a**, 63-70 (1996); received November 7, 1995

The structure of zinc chloride complexes with different ratios of chloride to zinc, formed in concentrated ZnCl₂ aqueous solutions, were determined from large-angle X-ray scattering using concentrations of the chloride complexes estimated by complementary Raman spectroscopic measurements. The highest chloro complex, $[ZnCl_4]^2$ -, is tetrahedral with a Zn-Cl bond length of 2.294(4) Å. The trichloro complex, $[ZnCl_3]^-$, which coordinates one water molecule, is pyramidal with the Cl-Zn-Cl angle 111°. The Zn-Cl and the Zn-H₂O bonds are 2.282(4) and 1.9 Å, respectively. The two lower complexes, $[ZnCl_2]$ and $[ZnCl]^+$, cannot be separated by Raman spectra. The average Zn-Cl distance in these complexes is 2.24 Å, and the average Zn-H₂O distance is 1.9 Å. In $[Zn(H_2O)_6]^{2^+}$ the Zn-H₂O distance is 2.15 Å.

Key words: X-ray diffraction; Raman spectra; IR spectra; structures of zinc (II) chloride complexes; structure of hydrated non-complexed zinc (II) ion.

1. Introduction

X-ray structure determinations of zinc (II) chloride complexes in strong aqueous solutions have been carried out by several investigators, and recently, their results have been summarized by Johansson [1]. In view of the results, the highest complex is $[ZnCl_4]^{2-}$, which has surely a tetrahedral structure. On the contrary, it appears that since, as stability constants suggest, the existence range of the complexes may overlap, the structures of the intermediate complexes, $[ZnX_n]^{(2-n)+}$ (n=1,2,3) have not been yet unambiguously determined. In these cases, it is essential to estimate the relative concentrations of the species which coexist with each other in sample solutions so that a more reliable knowledge of the structures of the complexes can be obtained.

Thus, in previous X-ray diffraction studies on zinc bromide and iodide complexes in aqueous solutions [2, 3], we have applied Raman and IR spectroscopies to the halide solutions to estimate the concentrations of the halide complexes in those solutions. According to the experimental results, in the hydrated Zn²⁺ ion the coordination is octahedral with the Zn-H₂O distance of 2.10 Å. The dibromozinc(II) complex, [ZnBr₂], has a bent structure with the Br-Zn-Br angle 115° and the Zn-Br distance of 2.38 Å, and the tribromozincate(II) ion is pyramidal with almost the same

angle and distance as those for the dibromo complex. The highest bromide complex, [ZnBr₄]²⁻, is tetrahedral with Zn-Br bond length of 2.405 Å, which is a little longer than those for the di- and tribromo complexes. Water molecules are probably coordinated to Zn in the di- and tribromo complexes, resulting in approximately tetrahedral structures, but unambiguous evidence for this could not be obtained. No structural information was obtained for the lowest bromide complex, [ZnBr]⁺. As for the zinc iodide system, the first iodide complex, [ZnI]⁺, is octahedral, but is changed into tetrahedral in the higher complexes, $[ZnI_2(H_2O)_2]$, $[ZnI_3(H_2O)]^-$, and $[ZnI_4]^{2-}$. The Zn-I bond length is 2.635 Å in the $[ZnI_A]^{2-}$ ion and slightly shorter, 2.592 Å in the two lower tetrahedral complexes. In the octahedral complex $[ZnI(H_2O)_5]^+$ the Zn-I bond length is 2.90 Å, much longer than those for the three higher complexes. Their Zn-H₂O bond distances in the iodide complexes are approximately the same as that in the hexaaquazinc(II) ion, 2.10 Å.

In the present work a similar investigation of the zinc chloride system was carried out. As was the case in the zinc bromide and iodide systems, Raman spectra were obtained for the zinc chloride solutions with approximately the same composition as that of the solutions for X-ray diffraction measurements so that the concentrations of the chloro complexes formed in each sample solution were estimated using the Raman bands corresponding to their symmetric stretching vibrations. IR spectra were also obtained for some zinc

Reprint requests to Dr. M. Maeda.

chloride solutions with the purpose of deducing whether the trichlorozincate(II) ion is trigonal planar or pyramidal.

2. Experimental

Preparation of Sample Solutions

Analytical grade zinc chloride and lithium chloride, the latter having been recrystallized twice from water, were dissolved in distilled water, and the solution was analyzed for Zn by complexometric titration and for Cl by gravimetry as AgCl. The composition (XAi and XBi) of the solutions for X-ray diffraction measurements is given in Table 1, and that for Raman and IR measurements (RA,..., RL) in Table 2.

X-Ray Scattering Measurements

The X-ray scattering from the free surface of the solution was measured with MoK radiation in a θ - θ

Table 1. Composition of the sample solutions for X-ray diffraction measurements.

	XA1	XA2	XA3	XB2	XB3
$Zn^{2+} (mol dm^{-3})$	7.488	5.010	2.867	1.618	0.9735
Cl-	14.98	15.02	14.04	4.977	4.428
Li+	_	5.00	8.30	1.74	2.48
H,O	38.82	36.65	37.83	49.94	50.26
$V(\mathring{A}^3)$	110.90	110.50	118.27	333.64	374.96
Zn(atoms/V)	0.50	0.33	0.20	0.33	0.22
Cl	1.00	1.00	1.00	1.00	1.00
Li	_	0.33	0.59	0.35	0.56
H,O	2.60	2.44	2.70	10.00	11.40
Cl-Zn ratio	2.00	3.00	4.90	3.01	4.55

Table 2. Composition of the sample solutions for Raman spectroscopic measurements (in mol dm⁻³).

	Zn ²⁺	Cl-	Li ⁺	ClO ₄	Cl ⁻ -Zn ²⁺ ratio
RA	3.13	1.73	=	4.52	0.55
RB	4.60	5.88	_	3.30	1.28
RC	2.64	5.18	-	0.10	1.96
RD	1.54	4.57	1.58	0.10	3.01
RE	1.09	4.60	2.52	0.10	4.22
RF	7.53	15.0	-	0.10	1.99
RG	5.02	14.9	4.92	0.10	2.97
RH	2.93	14.1	8.33	0.10	4.81
RI	2.06	14.8	10.8	0.10	7.18
RJ	-	5.03	5.03	-	_
RK	_	9.17	9.17	_	_
RL	-	12.7	12.7	_	-

diffractometer according to the analogous procedures to those described in [4]. A focusing LiF single crystal monochromater was positioned between the sample and the scintillation counter. The scattered intensity was measured at discrete points at θ -intervals of 0.1° for $1^{\circ}-20^{\circ}$ and 0.25° for $20^{\circ}-70^{\circ}$. Intensities below $\theta = 1^{\circ}$ could not be determined experimentally and were obtained by extrapolation to zero. Three different slit widths, 1/12°, 1/4°, and 1° were used to cover the complete range. For each point, 100 000 counts were taken, and each sample solution was scanned twice. The intensities for each slit combination were corrected for background radiation, which was determined by placing a lead plate just behind the receiving slit, and were normalized to the intensities measured with the 1° width slit from the data of overlapping regions.

Raman Measurements

For Raman spectroscopy, excitation was accomplished by using a single line of 514.5 nm wavelength from an Ar ion laser (NEC-GLG3200). The incident power was about 200 mW at the sample point. The sample solutions were contained in a cylindrical quartz cell with optically flat top and bottom. The Raman-scattered light was detected by a triple type monochromator (JASCO R-800T) equipped with a photomultiplier (Hamamatsu R-464) and a photon counter. The band path width of the monochromator was about 2 cm⁻¹.

Far-IR Measurements

Infrared spectra were measured in the range of 50 to 500 cm⁻¹ with a JEOL JIR-100 FT-IR spectrometer using a 6 mm Mylar beam splitter and a polystyrene windowed TDS detector. Platinum gauzes were used to contain the sample solutions. One hundred scanns at a resolution of 2 cm⁻¹ were accumulated for each solution.

3. Data Treatment

Raman Data

The Raman spectra of RA to RI were brought to a flat base by substraction of spectra of RJ, RK and RL (RA, RC, RD, RE – RJ; RB – RK; RF, RG, RH, RI – RL). The peak positions and areas under the peaks corresponding to the symmetric stretching vibra-

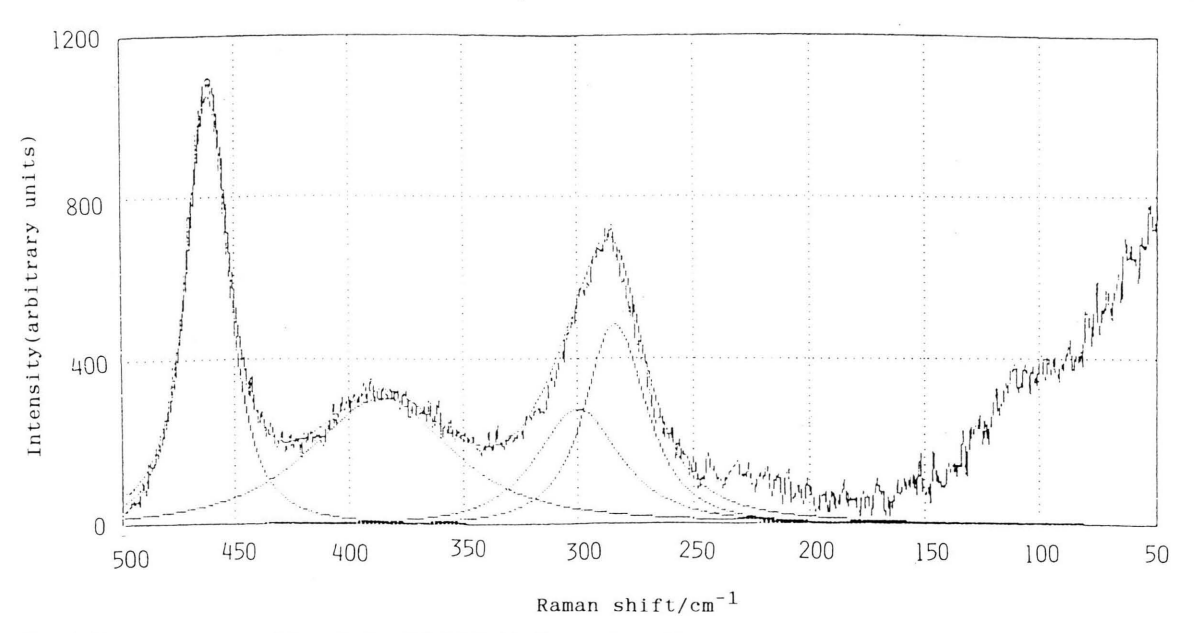


Fig. 1. Raman spectrum of the solution RA (cf. Table 2), together with resolved bands based on the horizontal background.

tion frequencies of the agua and chloro complexes of zinc(II) were estimated by curve fitting using Gauss-Lorentzian curve forms. An example is illustrated in Figure 1. The Raman bands having their maxima at 277, 283, 300, and 385 cm⁻¹ were assigned to $[ZnCl_4]^{2-}$, $[ZnCl_3]^-$, $[ZnCl_2]+[ZnCl]^+$, and $[Zn(H_2O)_6]^{2+}$, respectively, based on the available Raman data for ZnCl, aqueous solutions [5-7]. The bands for [ZnCl₂] and [ZnCl]⁺ could not be distinguished from each other. The polarized Raman band at 230 cm⁻¹, attributed to the presence of polynuclear aggregates [8, 9], was not observed in the present solutions. Only the [ZnCl₄]²⁻ complex was formed in RI solution, and the [ZnCl₃] - species was predominant in RE. A few complexes co-occurred in the other solutions. The areas under the peaks were normalized by using the v₁ (ClO₄) symmetric stretching band at about 934 cm⁻¹ as an internal standard.

The calculations of the concentrations of the aquaand chloro-complexes in those solutions were carried out according to the procedures described in [2] by assuming the concentration of each species to be proportional to the normalized area of its corresponding Zn-Cl or $Zn-H_2O$ stretching band. The concentrations of the complexes thus calculated in RA to RI solutions are tabulated in Table 3.

Table 3. Concentrations of aqua and chloro complexes of zinc(II) in the sample solutions for Raman spectroscopic measurements (in mol dm⁻³)

	$c([\mathrm{Zn}(\mathrm{H_2O})_6]^{2^+})$	$c([ZnCl]^+ + [ZnCl_2])$	$c([ZnCl_3]^-)$	$c([\operatorname{ZnCl}_4]^{2^-})$
RA	2.26	0.57	0.31	_
RB	2.33	1.13	1.13	_
RC	1.27	0.51	0.80	-
RD	0.30	0.38	0.82	-
RE	_	0.12	0.93	-
RF	2.25	2.40	2.61	-
RG	_	1.59	3.37	_
RH	_	_	0.80	2.08
RI	_	_	_	2.01

It is understood that RF, RG, RH, RD, and RE correspond approximately to XA1, XA2, XA3, XB2, and XB3, respectively, in solution composition. Thus it was assumed in the calculation of the concentrations of the complexes in the XA1 to XB3 solutions that the formation percentage of each complex is the same in the solutions for Raman- and X-ray-measurements corresponding with each other, and that the sum of the concentrations of the Zn(II) complexes is equal to the total concentration of zinc. The concentrations of the complexes thus estimated in the solutions for X-ray measurements are given in Table 4.

Table 4. Concentrations of chloro and aqua complexes of zinc(II) in the sample solutions for X-ray diffraction measurements (in mol dm⁻³)

	XA1	XA2	XA3	XB2	XB3
$\frac{1}{c([ZnCl_4]^{2^-})}$	_	_	2.07	_	_
$c([ZnCl_3]^-)$	2.69	3.41	0.79	0.88	0.86
$c([ZnCl]^{4}) + c([ZnCl_{2}])$	2.48	1.60	_	0.41	0.11
$c([Zn(H_2O)_6]^{2+})$	2.32	-	-	0.33	_

IR Data

The peak at 283 cm⁻¹ observed by the Raman measurements in solutions RE and RG, where the [ZnCl₃]⁻ complex is predominant, occurred also in the IR spectra. This fact suggests a non-planar (pyramidal) symmetry for [ZnCl₃]⁻.

Diffraction Data

The X-ray scattering data were treated by means of the KURVLR program [10] on a NEC PC-9801 DA personal computer. The measured intensities were corrected for polarization in the sample and monochromator, and for the absorption of the sample to give $I_{\rm obs}(s)$, where $s = (4 \pi/\lambda) \sin \theta$. The reduced intensities, i(s), were then calculated as

$$i(s) = K I_{\text{obs}}(s) - \sum_{i} n_i \cdot \{f_i(s)^2 + \text{del}(s) \cdot I_i^{\text{incoh}}(s)\}.$$
 (1)

K is a normalization constant chosen to refer all intensities to a stoichiometric volume containing one Cl atom in solutions. n_i is the number of atom "i" in the stoichiometric volume. The normalization was carried out by comparing observed intensity values in the high-angle part of the intensity curve $(\theta > 50^\circ)$ with the calculated sum of independent coherent and incoherent scattering. Scattering factors, $f_i(s)$, for neutral atoms were used with corrections for anomalous dispersion [11]. Values for incoherent scattering [11, 12] were corrected for the Breit-Dirac factors. The del(s) function is the fraction of the incoherent radiation reaching the counter, which was experimentally obtained.

The reduced intensities i(s) thus calculated are shown in Fig. 2 after being multiplied by s.

The radial distribution functions D(r) were calculated from

$$D(r) = 4 \pi r^2 \varrho_0 + 2 r / \pi \int_{0}^{s_{\text{max}}} s \cdot i(s) \cdot M(s) \cdot \sin(rs) \, ds,$$
 (2)

where $\varrho_0 = \left(\sum_i n_i Z_i\right)^2/V$, with Z_i the atomic number of i and V the stoichiometric unit of volume. The modification function M(s) was chosen to be $f_{2n(0)}^2/f_{2n(s)}^2 \exp{(-0.005 \, s^2)}$. The calculated radial distribution curves showed small spurious peaks in the range $<1 \, \text{Å}$, which can not be related to any interatomic distance. Thus, the reduced intensities were corrected for spurious peaks by means of the Fourier inversion of the radial distribution curve below $1 \, \text{Å}$ by taking into account the contributions from O-H interactions within H₂O.

The theoretical intensities due to interatomic interactions were calculated from

$$i(s)_{\text{calc}} = \sum_{i} \sum_{j} n_i f_i(s) f_j(s) \frac{\sin(r_{ij} s)}{r_{ij} s} \exp(-b_{ij} s^2),$$
 (3)

where r_{ij} and b_{ij} represent the distance and the temperature factor of the interaction between any atoms i and j, respectively.

Least-squares refinements of parameter values in the assumed structural model were made by minimizing the expression

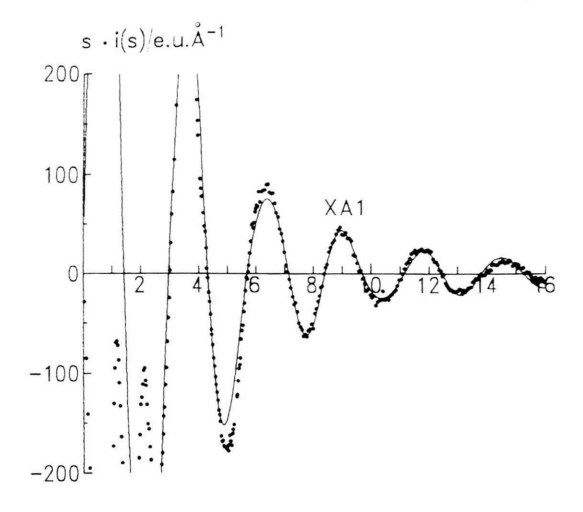
$$\sum s^2 [i(s)_{\text{exp}} - i(s)_{\text{theor}}]^2 \tag{4}$$

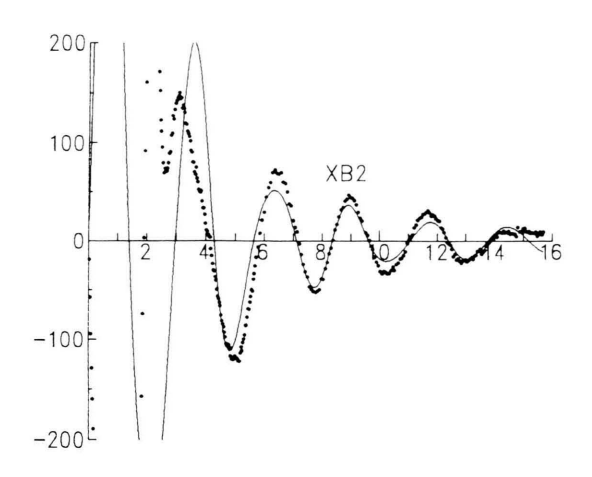
summed over the experimental s values.

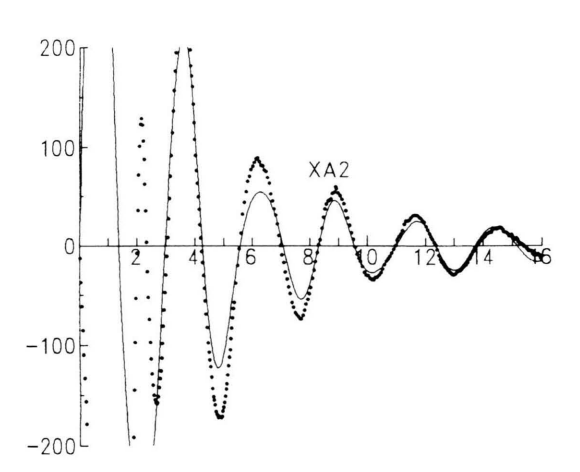
4. Results and Discussion

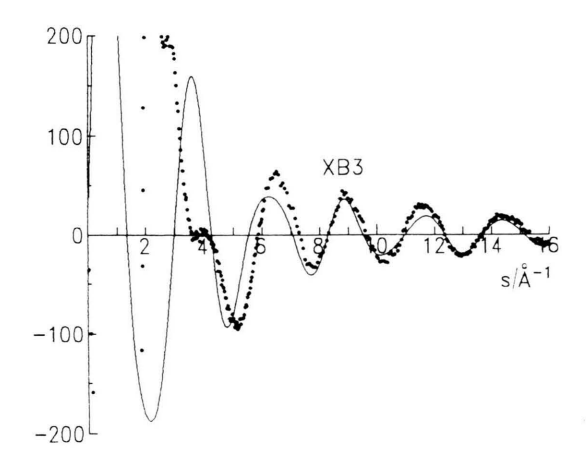
The radial distribution functions (RDF) are shown in Figure 3. The small peaks around 1.8 Å may result from interactions between Li⁺ and H₂O and also from those between Zn²⁺ and H₂O within the chloro complexes. The distinct peaks at about 2.3 Å are attributed to Zn-Cl bonds within the chloro complexes, and to Zn-OH₂ bonds within the aqua-complex according to the previous X-ray investigations of aqueous zinc(II) solutions. The third peaks at 3.8 Å which appear in the XA solutions may be due to Cl-Cl interactions within the chloro complexes. The broad peaks in the XB solutions appear in the region 3-4 Å, which may correspond to both the distance between the chloride ions and neighboring water molecules, and the Cl-Cl distances within the chloro complexes.

The intramolecular distances (r's) and corresponding temperature factors (b's) for [ZnCl₄]² and [ZnCl₃]⁻ were determined by least squares refinements of the high-angle parts of the intensity curves using values for the concentrations as estimated from the Raman spectra. A too low cut-off limit for the









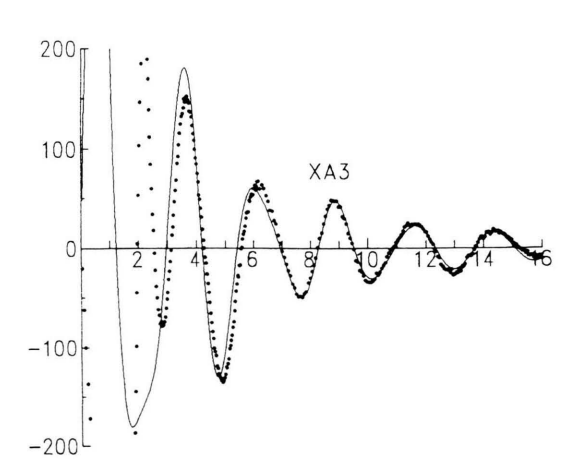


Fig. 2. Comparison between observed (dotted line) and calculated (solid line) $s \cdot i(s)$ for the atom pairs concerned, using their parameter values indicated in the text. For XAi and XBi cf. Table 1.

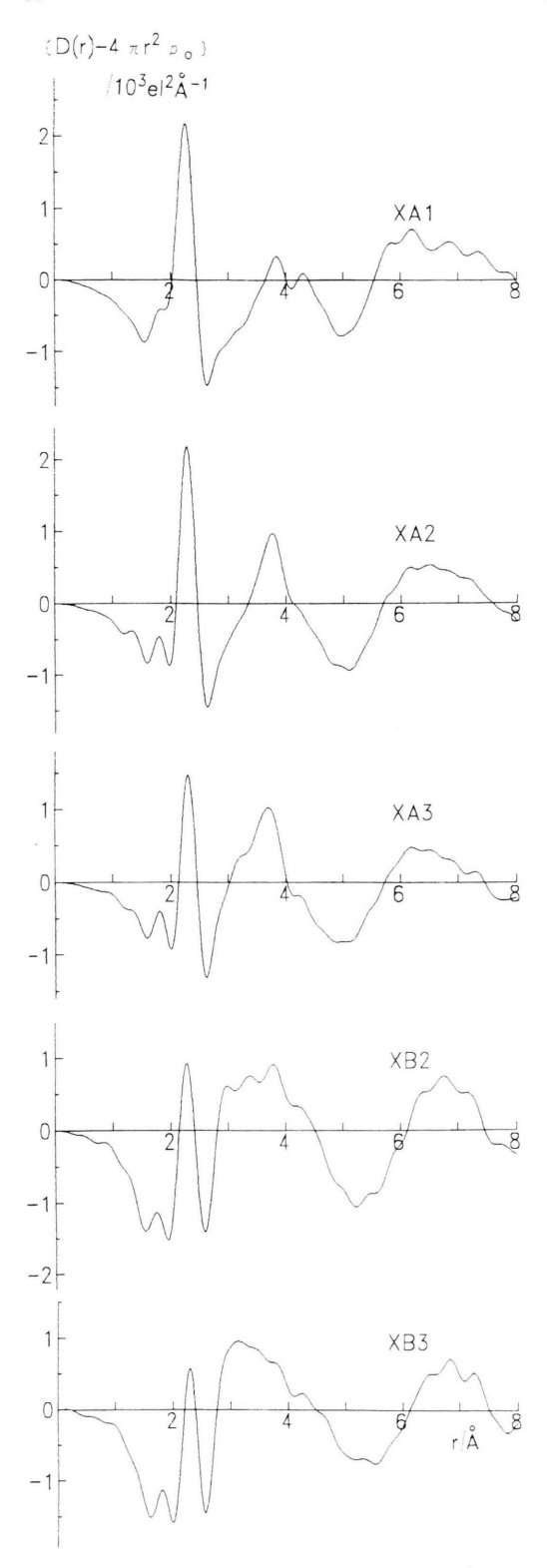


Fig. 3. Radial distribution curves, $D(r) - 4\pi r^2 \varrho_0$.

range of s values used in a refinement will increase contributions from unknown intermolecular interactions and result in systematic errors in the parameters obtained. A too high cut-off limit, on the other hand, will lead to larger uncertainties in the results because of too few experimental data. The least squares refinements were, therefore, carried out using different values for the lower s limit, and the results were checked for constancy in the parameter values obtained.

For [ZnCl₄]²⁻, the parameter values were determined from the XA3 solution in which [ZnCl₄]²⁻ is assumed to be the predominant complex. Intensity data for the XA2 and XB3 solutions were used for the structure determination of [ZnCl₃]⁻. In the first series of refinements, minor complexes present were ignored but were included in successive refinements, when their structures became known. The intramolecular distances and temperature factors for [ZnCl₄]²⁻ thus determined were

$$r_{\text{Zn-Cl}}/\text{Å} = 2.294(2), \ b_{\text{Zn-Cl}}/\text{Å}^2 = -0.0003(2);$$

 $r_{\text{Cl-Cl}}/\text{Å} = 3.69(2), \ b_{\text{Cl-Cl}}/\text{Å}^2 = 0.015(2),$

and those for [ZnCl₃] were

$$r_{\text{Zn-Cl}}/\text{Å} = 2.282(2), \ b_{\text{Zn-Cl}}/\text{Å}^2 = 0.0001(2); r_{\text{Cl-Cl}}/\text{Å} = 3.76(1), \ b_{\text{Cl-Cl}}/\text{Å}^2 = 0.007(1),$$

from XA2 and

$$r_{\text{Zn-Cl}}/\text{Å} = 2.281 (5), \ b_{\text{Zn-Cl}}/\text{Å}^2 = -0.0001 (2);$$

 $r_{\text{Cl-Cl}}/\text{Å} = 3.76 (3), \ b_{\text{Cl-Cl}}/\text{Å}^2 = 0.009 (2)$

from XB3. The results for $[ZnCl_4]^{2^-}$ showed that the ratio between the Zn-Cl and the Cl-Cl distances did not differ significantly from that expected for a tetrahedral structure. For $[ZnCl_3]^-$, the Zn-Cl and the Cl-Cl distances determined from the XA2 and the XB3 solutions, respectively, were the same within the standard deviations. The Zn-Cl bond is slightly shorter and the Cl-Zn-Cl bonding angle (111°) is slightly larger than those in the tetrahedral $[ZnCl_4]^{2^-}$ complex. These results are analogous to those found previously for other zinc halide complexes [2, 3].

The structure of the hydrated non-complexed Zn^{2+} ion was determined by taking the difference between the RDF's for the XA1 solution in which the hydrated non-complexed Zn^{2+} ions are predominant, and the XA2 solution after subtracting the $[ZnCl_3]^-$ contributions (see Figure 4). In the resulting difference curve (solid line) the $Zn-H_2O$ distances should give a dominant peak, which is in close agreement with a calculated peak for six $Zn-H_2O$ interactions at 2.15 Å (see the broken curve obtained by subtraction of the

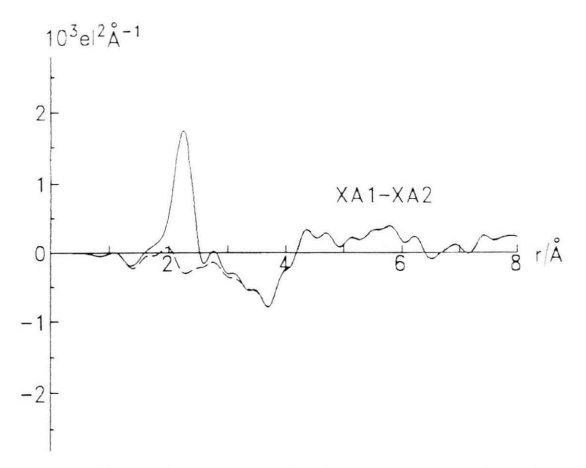


Fig. 4. The difference curve (solid line) between the D(r)'s for the XA1 and XA2 solutions obtained after subtracting the $[ZnCl_3]^-$ contributions. The curve (broken line) is obtained by subtracting the $[Zn(H_2O)_6]^{2+}$ contributions from the difference curve (solid line).

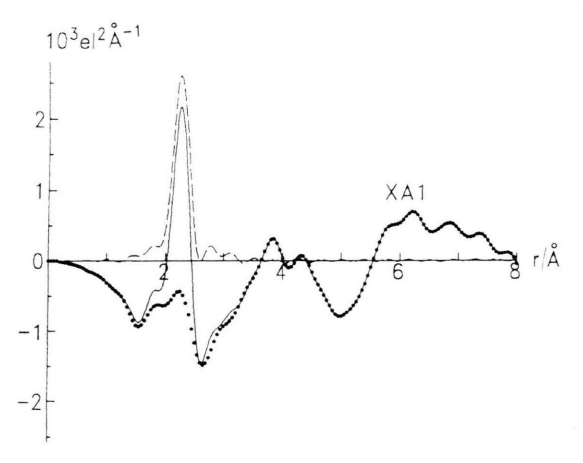


Fig. 5. The difference curve (dotted line) obtained by subtracting the contributions (broken line) due to Zn–Cl and Zn–OH₂ interactions within [ZnCl₃]⁻ and [Zn(H₂O)₆]²⁺, respectively, from the $D(r)-4\pi r^2 \varrho_0$ (solid line) curve for XA1

 $[Zn(H_2O)_6]^{2+}$ contributions from the difference curve (solid line) in Figure 4). The distance obtained in the present system is within 2.08-2.17 Å determined by X-ray diffraction of aqueous solutions of various zinc(II) salts [1].

The XA1 and XB2 solutions contain the largest relative concentrations of the lower complexes [ZnCl₂] and [ZnCl]⁺. For a derivation of their structures the contributions due to Zn-Cl and Zn-OH₂ interactions within [ZnCl₃] and [Zn(H₂O)₆]²⁺, respectively, (contributions from aqua Li⁺ ions which were assumed to have a tetrahedral coordination with Li⁺-H₂O distances of 1.9 Å being also subtracted from the RDF for the XB2 solution) were subtracted from the D(r)'s for XA1 and XB2. In the resulting difference curves (see the dotted curve in Fig. 5 for XA1) peaks occur at 2.25 Å and 1.9 Å. The first peak stems obviously from a Zn-Cl bond, which is slightly shorter than those in the higher complexes. The second peak is interpreted to correspond to Zn-H₂O distances within the complexes including [ZnCl₃]⁻. The Zn-H₂O bonds within the complexes are shorter than those (2.08-2.17 Å) within the hydrated noncomplexed Zn^{2+} ion, $[Zn(H_2O)_6]^{2+}$. This tendency is also observed in crystals. That is, a discrete tetrahedral complex [ZnCl₃(H₂O)] has been found in crys-

tals of KZnCl₃ (H₂O)₂, in which the Zn-OH₂ bond distance is 2.02 Å [13]. The Zn(II) ion in crystal hydrates has a regular octahedral structure, and the Zn-OH₂ distances are in the range of 2.08-2.14 Å [14]. There is no clear indication of any longer Zn-Cl bond, which would be expected, as is the case for octahedral [ZnI(H₂O)₅]⁺ complex in aqueous solution [3] and octahedral [ZnCl₂(H₂O)₄] complex in crystals of ZnCl₂ 11/3 H₂O [15], if an octahedral [Zn- $Cl(H_2O)_5$ complex rather than a tetrahedral one were present. Since the Raman spectra can not be used to separate the concentrations of [ZnCl]+ and [ZnCl₂], no definite conclusion about the coordination in [ZnCl]⁺ can be made. The four-coordination may be retained in the [ZnCl] + complex, or its concentration may be too low to give sufficient contributions to the diffraction data.

In Fig. 2 the observed si(s) values are compared with those calculated for the atom pairs concerned using their parameter values. The agreement is good especially for XA solutions, in which the concentrations of the complexes are much higher than those in XB solutions, except at low s regions where various interactions including intermolecular interactions, which are not taken into account in the present calculations, significantly contribute to the $s \cdot i(s)$ values.

- [1] G. Johansson, Advances in Inorganic Chemistry, ed. A. G. Sykes, Academic Press, San Diego 1992, vol. 39, pp. 159–232.
 [2] P. L. Goggin, G. Johansson, M. Maeda, and H. Wakita,
- Acta Chem. Scand. A38, 625 (1984).
- [3] H. Wakita, G. Johansson, M. Sandström, P. L. Goggin, and H. Ohtaki, J. Solution Chem. 20, 643 (1991). G. Johansson, Acta Chem. Scand. 20, 553 (1966).
- [5] M. L. Delwaulle, Bull. Soc. Chim. France 1294 (1955).
- [6] D. F. C. Morris, E. L. Short, and D. N. Waters, J. Inorg. Nucl. Chem. 25, 975 (1963).
- [7] J. W. Macklin and R. A. Plane, Inorg. Chem. 4, 821
- [8] D. E. Irish, B. McCaroll, and T. F. Young, J. Chem. Phys. 39, 3436 (1963).

- [9] G. Gali, S. Magazu, D. Majolino, P. Migliardo, M. C. Bellissent-Funel, F. Allota, and C. Vasi, Nuovo Cimento D 12, 197 (1990).
- [10] G. Johansson and M. Sandström, Chem. Scripta 4, 195 (1973).
- [11] D. T. Cromer, J. Chem. Phys. 50, 4857 (1969).
- [12] D. T. Cromer and J. B. Mann, J. Chem. Phys. 47, 1892
- [13] P. Süsse and B. Brehler, Beiträge Mineral. Petrograp. 10, 132 (1964).
- [14] J. Burgess, Ions in Solution Basic Principles of Chemical Interactions, Ellis Horwood, Chichester 1988, Chapt. 3.
- [15] H. Follner and B. Brehler, Acta Crystallogr. B26, 1679 (1970).